

## Continuous-wave phase-sensitive parametric image amplification

S. GIGAN, L. LOPEZ, V. DELAUBERT, N. TREPS, C. FABRE and A. MAITRE

(Received 00 Month 200x; In final form 00 Month 200x)

We study experimentally parametric amplification in the continuous regime using a transverse-degenerate type-II Optical Parametric Oscillator operated below threshold. We demonstrate that this device is able to amplify either in the phase insensitive or phase sensitive way first a single mode beam, then a multimode image. Furthermore the total intensities of the amplified image projected on the signal and idler polarizations are shown to be correlated at the quantum level.

### 1 Introduction

Parametric interaction is widely used in quantum optics, because it is a very useful tool to produce quantum correlated and entangled light. In most cases, only temporal or polarization aspects of entanglement or squeezing are used [1]. But the parametric process also produces spatial quantum entanglement [2] which can be useful in many applications, for example in two-photon or “ghost” imaging [3], a subject which has recently aroused a great interest in the community.

Due to the low parametric coupling in crystals, experiments with parametric crystals are usually operated in the photon-counting regime, or require the high peak power of pulsed lasers. However many applications, such as high sensitivity measurements below shot noise, require intense non-classical c.w. beams: instead of single pass parametric interaction, one then prefers Optical Parametric Oscillators which produce quantum-correlated laser-like beams [4]. Usually the cavity used for the OPO is resonant for a single transverse mode of the field and acts as a perfect spatial filter. In order to obtain imaging effects in OPOs, one needs cavities which are simultaneously resonant on many transverse modes, the so-called transverse-degenerate cavities, such as the concentric, confocal or hemi-confocal cavities. Classical multimode effects, such as pattern formation, have been observed in transverse degenerate OPOs [5].

arXiv:quant-ph/0502116v2 [20 Feb 2005]

Quantum spatial effects in OPOs have been the subject of many theoretical papers [6, 7]. As far as experiments are concerned, the first multimode non-classical effect observed in OPOs has been reported in [8]. By measuring the transverse distribution of correlations between the signal and idler beams emitted by a confocal OPO above threshold, it was experimentally shown that this device generated a non-classical multimode beam.

The present paper reports experimental results obtained in a frequency degenerate OPO operating below the oscillation threshold. The aim of the experiment is to use a transverse-degenerate OPO to amplify a weak injected image in a phase-sensitive way, in order to realize noiseless amplification and quantum cloning of the original image. This work is an extension to the c.w. regime to what has been already observed in the pulsed, single pass regime [9, 10]. It presents the first experimental achievements obtained with this device: observation of c.w. single-mode and multimode parametric amplification at the classical and quantum level.

The paper is organized as follows: after a short reminder of the main features of type II parametric amplification, section III reports on the observation of single-mode amplification of a weak injected signal in the phase sensitive configuration, first using a scanned cavity, then in a locked cavity configuration. It then describes a new set-up based on a dual-cavity, where pump and signal-idler resonate in different cavities, and show that stable phase-sensitive amplification is obtained in this device. In section IV, we demonstrate multimode amplification of an image made of a double slit with the same system operating in a hemi-confocal configuration, and show finally the existence of quantum correlations between the total intensities of the signal and idler amplified images.

## 2 Properties of type II, frequency degenerate, Optical parametric Amplification

Let us consider a type II parametric interaction where the signal and idler modes have the same frequency  $\omega$  and are respectively polarized along the  $Ox$  and  $Oy$  axes. A weak field of the same frequency  $\omega$  injected in such a device is predicted to be amplified at the output of the crystal. If the input field polarization is aligned either along the  $Ox$  or  $Oy$  axis, the amplification is phase insensitive and therefore inevitably adds noise to the input field. The signal to noise ratio is deteriorated by a factor equal to 2 in the high gain limit. In contrast, when the input field is injected at 45 degrees from these axes, the amplification is phase sensitive: there is either amplification or de-amplification, depending on the relative phase between the pump wave at  $2\omega$  and the injected wave [11]. In the ideal case, there is no noise added in the

latter configuration: the amplification is said to be noiseless. Furthermore, if one decomposes the output field on its two polarization components along the signal and idler polarization axes  $Ox$  and  $Oy$ , one gets two intensity correlated outputs, which are in some respect two "quantum clones" [12]. These effects have already been experimentally demonstrated [11] for a single transverse mode input field in single pass amplification using an intense pulsed laser as a pump. To extend it to the domain of continuous wave fields, one puts the crystal in a resonant cavity and go to the "regenerative parametric amplification" regime, with a gain tending to infinity when one approaches the oscillation threshold of the Optical Parametric Oscillator from below. The modulation bandwidth of this amplifier is reduced with respect to the single pass amplifier, and restricted to the optical cavity bandwidth. At the quantum level [13], the intracavity parametric amplifier has essentially the same properties as the single pass one: possibility of noiseless amplification and quantum cloning. Finally, if one wants to reduce the threshold, in order to be able to pump the system high above threshold with moderate powers and excite at the same time many transverse modes, it is better to use a triply resonant OPO, where the signal, idler and pump modes are simultaneously resonating.

### 3 Single mode c.w. optical amplification

#### 3.1 *Experimental Setup*

The experimental setup is an upgrade of the one described in [8] (figure 1). We start from a very stable Nd-YAG master laser from InnoLight, delivering 1.2W single-mode continuous output power at 1064 nm, which is used to inject and stabilize a flash-lamp-pumped ring-cavity Nd-YAG "slave" laser. This configuration gives a stable single-mode beam of up to 6W at 1064 nm. A part of it is injected into a semi-monolithic frequency doubling cavity, using a MgO:LiNbO<sub>3</sub> crystal, which produces up to 1.7 W of 532nm green light, used as a pump beam for the OPO. The remaining part is injected into an impedance-matched ring Fabry-Perot cavity used as a spatial filter ("mode cleaner"), and used to inject the amplifier. An object, such as a slide or a resolution target, can be placed in the beam. With this system it is possible to obtain 1.2W at 532 nm for pump, and simultaneously and 1W at 1064 nm for injection. The phase between the pump and the injection is controlled by mirror placed on a piezo-electric transducer.

The different optical cavities are stabilized using the Pound-Drever-Hall method [16]. For this purpose three electro-optic phase modulators (EOM) are inserted in the beam path. EOM1 adds a phase modulation at 14.7MHz on the infrared beam and allows to lock the slave laser, the doubling cavity and the spatial filtering cavity. EOM2 adds a phase modulation at 19 MHz

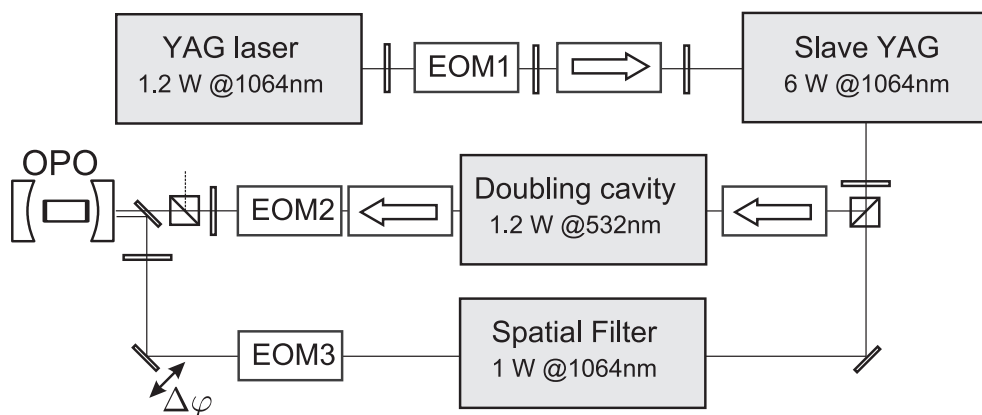


Figure 1. Source system for amplification.

on the pump beam to lock the OPO on a pump resonance. EOM3 modulates at 16.5 MHz the infrared injection beam to stabilize the OPO on a signal or idler resonance.

The detection scheme is represented on figure 2: a dichroic mirror (DM) rejects the residual green light from signal and idler modes. The reflected pump is sent onto a photodiode ( $D_G$ ) to monitor the OPO and to stabilize it. Signal and idler beams are separated by a polarizing beam splitter and sent to two InGaAs photodetectors ( $D_1$  and  $D_2$ ), having matched quantum efficiencies within better than 1% and equal to  $90\% \pm 5\%$ . A flipping mirror (FM) with approximately 50% reflection diverts some of the intensity of the signal and idler beams onto an imaging set-up, which allows us to simultaneously record on a CCD camera the signal and idler transverse intensity distributions. A secondary flipping lens (FL) is used to switch between two configurations: in the first one, the CCD plane is the conjugate plane of the crystal center plane ("near field"); in the second one, one monitors on the CCD the Fourier transform of the previous one ("far field").

The data acquisition system relies on computer storage of the quantum fluctuations: the photocurrent, amplified by a low-noise 36dB broadband transimpedance amplifier, is mixed with a current oscillating at frequency  $5MHz$  and filtered on a  $100kHz$  low-pass filter. Together with the DC photocurrents, the high frequency signals are then recorded by an acquisition card (PCI6110E from National Instrument), which stores in four 12-bit channel at a rate of 200 kHz the DC and the demodulated HF parts of each photocurrent. A post-processing treatment of the data allow us first to calibrate the shot noise level and then to obtain normalized noise variances on the signal and idler photocurrents normalized to shot noise, together with their normalized correlation function.

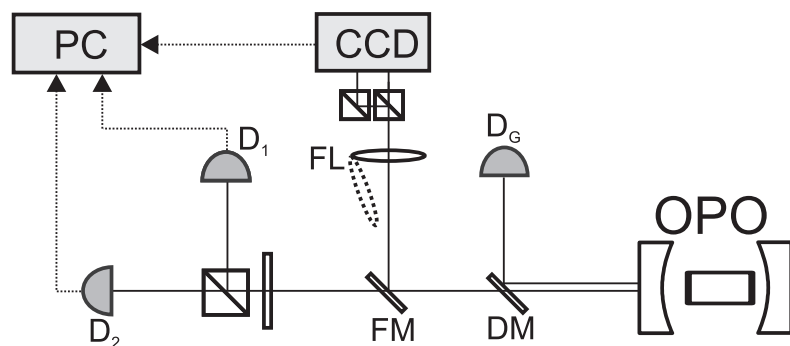


Figure 2. detection scheme.

### 3.2 Single mode amplification in a nearly confocal cavity

We use a walk-off compensated KTP crystal cut for non-critical type-II colinear phase-matching and frequency degeneracy. Its temperature is electronically stabilized around  $33\text{ }^{\circ}\text{C}$  within 1 mK. The cavity is made by two mirrors with radii of curvature  $R = 100\text{ mm}$ , separated by a distance of approximately 100 mm, i.e. close to confocality, but not exactly tuned to it. The input coupler reflects 90 % of the 532 nm light, and almost all the 1064 nm light. The output coupler reflects almost all the 532 nm light, and 99% of the 1064 nm light. The oscillation threshold of this OPO is approximately 20 mW. The operating point is taken as close as possible to the threshold for higher parametric gain.

Both pump and injection are spatially matched to the  $TEM_{00}$  cavity mode, and a half-wave plate allows us to rotate the polarization of the injection beam, and to inject it on a chosen polarization direction. As the refractive indices for signal, idler and pump (respectively 1.8296, 1.7467 and 1.7881) are different, the three modes do not in general resonate for the same length of the cavity. Triple resonance is achieved by precisely tuning various cavity parameters. A fine temperature tuning gives simultaneous resonance of signal and idler modes. The temperature range to get it is approximately 20 mK, within our regulation stability range. Tilting the crystal allow us to reach the triple resonance configuration. Only a very slight tilt is possible without deteriorating the optical alignment of the cavity.

This method has allowed us to observe a strong amplification in the phase insensitive configuration (injection along the signal or idler polarisation), while sweeping the cavity length through the triple resonance point. We have measured a maximum gain in such a "transient" c.w. Optical Parametric Amplifier of  $23\text{ dB}$ .

We have then rotated the injected field polarization by 45 degrees and stabilized the OPO length on the triple resonant point. By scanning the relative

phase between the pump and the injected field, we have observed phase sensitive amplification with gain up to 6dB (figure 3) on time scales of the order of a few seconds. To our knowledge, this is the first observation of such an effect in the c.w. regime and in a type II configuration. The gain value is smaller than in the scanned configuration, because of crystal heating effects which appear when the cavity is locked and bring the signal and idler modes out of resonance, and also because exact and stable triple resonance is difficult to obtain. As can be seen on figure 3, the signal and idler beams do not have the same mean intensity because the idler mode is not perfectly resonant. This problem of triple resonance is very similar to the problem of frequency degenerate operation of an OPO above threshold [15,14].

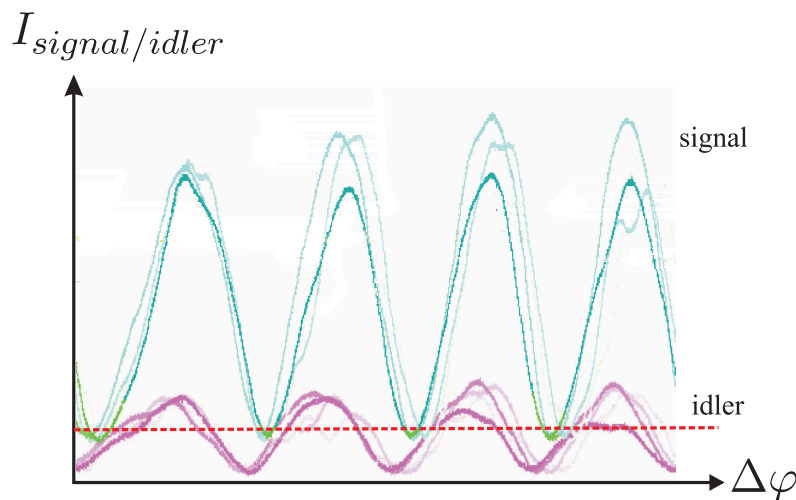


Figure 3. Signal and idler intensities as a function of the relative phase between the injected  $TEM_{00}$  mode and the pump mode. The input field polarization is at 45 degrees from the cavity optical axes. The dashed line is the signal and idler intensity without amplification.

### 3.3 Single mode amplification in a dual cavity

To solve the stability problems we have used a new setup, based on a dual cavity configuration, in which the signal and idler modes resonate in a different cavity from the pump cavity, but where the three modes overlap in the crystal. To our knowledge this kind of cavity has been introduced and realized for the first time in [17], and has been used in a c.w. OPO in [18] to produce twin beams, in the pulsed regime [19] to emit single mode beams or to produce mode-hop free continuously tunable OPO [20].

The linear dual cavity is shown in figure 4. The pump cavity is limited

by mirrors M1 and M3, and the signal-idler cavity by mirrors M2 and M4. The characteristics of these mirrors are summarized in table 1. Both cavities are approximately 50mm long, and the 10mm-long KTP crystal is cut for frequency degenerate operation, and non-critical phase-matching, but is not walk-off compensated. The advantage of such a dual cavity is that it is now possible to control and stabilize independently the length of each cavity. The triple resonance condition is then obtained by temperature tuning, and is much more stable. M2 and M3 being parallel, the parallelism of the optical axes of the two cavities is automatically ensured. The coincidence of these axes is finally adjusted, by slightly tilting the mirrors M1 or M4 to maximize the mode overlap, so as to obtain the minimum threshold possible, of the order of  $30mW$ .

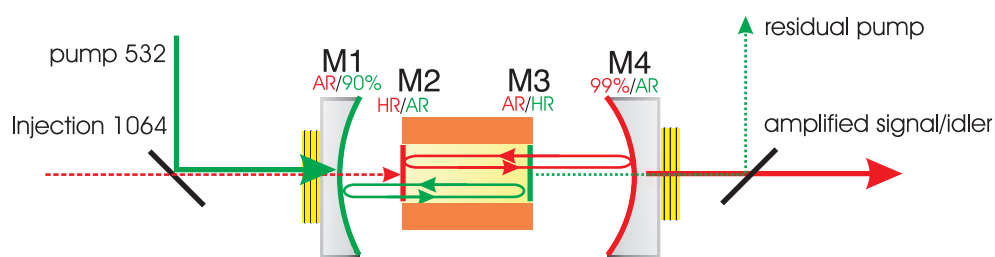


Figure 4. Scheme of the dual-cavity.

	M1	M2	M3	M4
Radius of curvature	100mm	plane	plane	100mm
reflectivity at 532nm	90%	5.25 %	99.3 %	6.6%
reflectivity at 1064nm	5%	99.96 %	0.11 %	98.93 %

Table 1. characteristics of the mirrors of the dual cavity

Because of the imperfect antireflection coatings deposited on the crystal faces, unavoidable with dual-wavelength coatings, the M1-M2 and M3-M4 systems constitute low finesse secondary cavities. This implies in particular that the intracavity pump signal and idler powers depend also on the resonance condition of these cavities, so that it is difficult to know the exact power of the modes circulating in the cavity.

When the dual cavity is injected at  $45^\circ$  of the crystal axes, and when the pump and injected modes are the  $TEM_{00}$  modes of their respective cavities, we have measured below the oscillation threshold c.w. stable phase-sensitive amplification with typical gains of 5-6 dB (figure 5). The precise gain value is not known because of the secondary cavity effect. Let us note that in this new

set-up, the signal and idler modes have the same intensity, and that it remains stably on the triple resonant point during several minutes. It was not possible to observe higher gains because the intracavity pump intensity variations due to the secondary cavity prevented us from operating very close to threshold.

When one removes mirror M1, one obtains a doubly resonant OPO, having an oscillation threshold around  $200mW$ . We have also observed phase sensitive amplification with typical gain of 4-6dB in this configuration. We have evaluated finally the quantum correlation between the intensities of the signal and idler components of the amplified output beam : for a parametric gain of the order of 6dB, the noise on the difference between the two intensities has been measured 35 % below the standard quantum limit. These results are consistent with the expected performance of the cavity and of the detection scheme, taking into account losses and quantum efficiency.

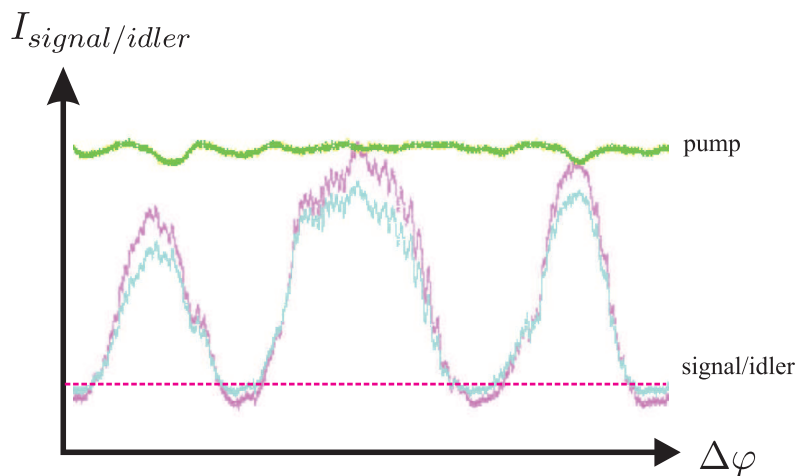


Figure 5. Signal and idler intensities as a function of the relative phase between the injected  $TEM_{00}$  mode and the pump mode. The input field polarization is at 45 degrees from the cavity optical axes. The geometry of the dual cavity is close to hemi-confocal. The dashed line is the signal and idler intensity without amplification.

## 4 multimode amplification

### 4.1 Experimental setup

The previous set-up has been modified for multimode image amplification: by using a mirror M1 having a large radius of curvature, the pump cavity  $TEM_{00}$  mode has a larger waist, and is likely to pump many transverse modes of the signal-idler cavity. This latter cavity is then brought to an exact transverse



degenerate configuration. Because of the plane surfaces of the mirrors M2 and M3 deposited on the crystal faces, we have been compelled to use the hemi-confocal configuration, in which the concave mirror is separated from the plane mirror by a distance equal to half its radius of curvature. More precisely, we chose a radius of curvature for M1 of 2000mm and a length of 50 mm, which gives a waist for the pump cavity of  $250 \mu\text{m}$ . The signal-idler cavity had a M4 mirror of radius  $R = 100\text{mm}$ . In the hemi-confocal configuration, this gives a waist of  $120 \mu\text{m}$ . The pump waist is therefore twice as big as the signal-idler waist.

The injection system was also modified. The  $TEM_{00}$  mode coming out of the mode-cleaner was focussed into the OPO infrared cavity with a waist size equal to three times the cavity waist. In the transverse plane which is the reciprocal image of mirror M2 surface (which is the location of the minimum waist of the cavity mode), we placed a black and white transmission pattern (USAF resolution target, consisting of various horizontal or vertical slit, numbers, squares). The field injected in the cavity is therefore the image of the object chosen on the target multiplied by a gaussian intensity envelope.

## 4.2 Results

The hemi-confocal cavity is not an exact self-imaging cavity [21], meaning that all the transverse modes do not resonate at the same length. Even without a nonlinear crystal inserted in it, it is not a "transparent device", as it does not perfectly transmit any input image. Its behavior in terms of image transmission has been studied in detail in [22]. It can be described as follows : one finds four cavity resonances when scanning the cavity length over a range  $\lambda/2$ . At each resonance length, the cavity is resonant for one quarter of the transverse modes. For example, if the cavity length is stabilized on the resonance of the mode family containing the  $TEM_{00}$  mode, it transmits the even part of the input image plus the even part of its spatial Fourier transform.

As an example, figure 6 shows the intensity patterns recorded by the CCD camera on the signal and idler modes transmitted through the "cold" hemi-confocal cavity (without pump light). The input object is a "6" slightly shifted from the cavity optical axis and injected with a polarization at 45 degrees from the signal and idler polarizations. One observes at the output of the cavity an image looking like a "69", multiplied by a gaussian envelope limiting the field of view to the image center, plus a bright pattern at the center: this complex feature corresponds indeed to the even part of the input ("69") plus its spatial Fourier transform (central part). Looking more precisely at the signal and idler components of the output, one notices an effect due to the walk-off: the transmitted image is slightly different in the signal and idler beams. The "6" and the "9" are exactly symmetric with respect to the central feature in the

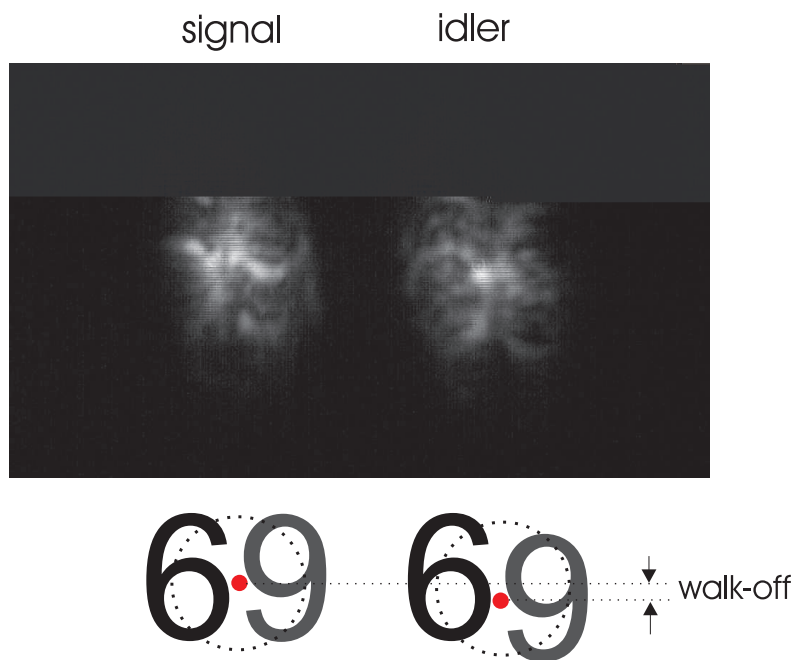


Figure 6. Above: signal (left) and idler (right) images transmitted through a hemi-confocal cavity without pump when an object consisting of an off-axis "6" is injected in the cavity. Below: sketch of the obtained pattern, indicating the optical symmetry axis (central dots) and the waist size of the mode used to illuminate the object (dashed circles), giving a kind of "field of view" in this experiment, as the outer parts of the transmitted image cannot be seen outside this circle

signal beam and have a small lateral shift in the idler beam. This is due to the fact that, because of the walk-off, the cavity axis is not exactly the same inside the crystal for signal and idler.

Taking a simpler image having the shape of a double slit (multiplied by a Gaussian envelope) sent with a polarization at 45 degrees from the signal and idler polarizations, we have observed what is, to the best of our knowledge, the first phase-sensitive amplification of an image in the c.w. regime, as can be seen on the total signal and idler intensities plotted on figure 7 as a function of the relative phase between the injected signal and the pump. From the constant value of the transmitted pump and the almost equal values of the signal and idler intensities, one notices that the triple resonance condition is well satisfied during the whole recording. We have been able to stabilize for the few seconds the relative phase on the maximum and minimum amplification points using the transmitted signal-idler modulation amplitude at 19.5MHz (due to the corresponding pump modulation created by EOM2) as an error signal. This has enabled us to record the whole transmitted image with the CCD camera at the intensity maximum and minimum. These two images, on

the right side of figure (7), are both roughly identical to the transmitted image without amplification, that is not represented in the figure, but with different intensities. Like in the example of figure (6) they consist of the even part of the object (the slit double itself in the present case) plus the vertical three dot pattern which is central part of the Fourier transform of the horizontal double slit. This last feature is here the most intense part of the image because it is concentrated in the central part of the transverse plane and is less affected by the overall multiplication by the Gaussian beam shape.

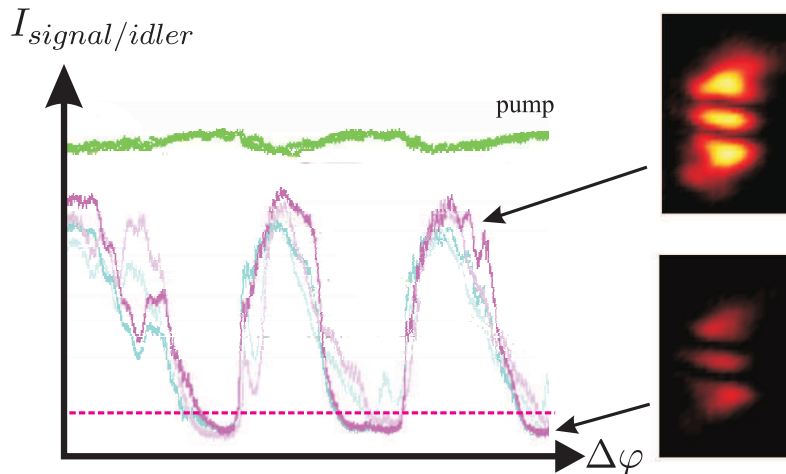


Figure 7. Left side: pump, signal and idler total intensities as a function of the relative phase between injected mode and pump mode. The dashed line is an estimation of the signal and idler intensity without amplification. Right side: transverse profile of the signal beam at maximum and minimum amplification.

By performing a point by point division of the two images, we obtain an estimation of the local gain and of its spatial variation. The result is represented on figure 8. For the same reasons as in the single mode case, it is not possible to deduce from the data an exact value of the gain. One notices that the calculated quantity is roughly homogeneous, with a mean value close to 3 (5dB) over all the area where the local intensity of the image has a significant value. The size of the  $TEM_{00}$  cavity mode is indicated by the black circle. The fact that one gets significant amplification well beyond the extension of this fundamental mode is another indication of the multimode character of the present amplifier.

Finally we have found evidence of quantum correlations between the signal and idler components of the amplified image. We have observed that the noise level on the difference between the total intensities of the signal and idler beams is 12 % below the shot noise limit when the image mean intensity

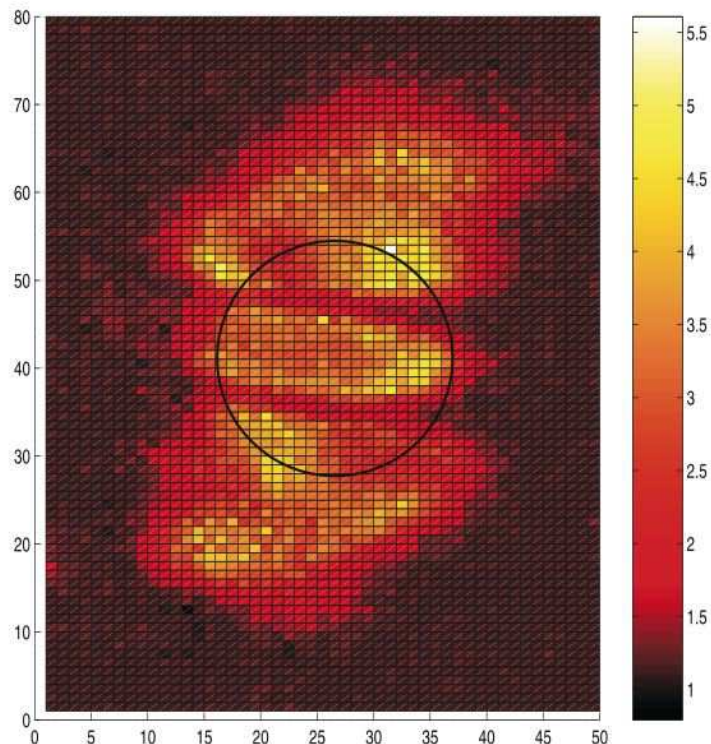


Figure 8. Spatial variation of the ratio between the transmitted images on the signal beam taken at the points corresponding to the maximum and minimum total intensities. The circle indicates the size of the  $TEM_{00}$  cavity mode

reaches its maximum value. The reason why the quantum correlation turns out to be smaller for the image amplifier than for the single mode amplifier at comparable gains is unknown at the moment.

## 5 Conclusion

We have studied intracavity optical parametric amplification in the c.w. regime, and obtained first results on a system which has not received so far a great deal of attention, in spite of its promising possibilities: evidence for single-mode phase sensitive c.w. optical amplification with a significant gain in scanned cavity configuration, observation of phase sensitive single mode amplification in the quantum cloning regime, and more importantly first evidence of c.w. phase sensitive amplification of simple images, also in the quantum cloning regime.

These are encouraging first results which need to be improved and investigated further. It would be in particular interesting to determine the noise figure, and its spatial variation of this amplifier. Let us note that the present set-up was not optimized for single mode amplification, and that even better gain values and more important quantum correlations could be obtained in a more optimized configuration of finesse and cavity transmission factors. Such an optimized system could also be used as a noiseless amplifier.

As far as quantum imaging effects are concerned, the present set-up does not enable us to look for local quantum correlations and local squeezing because of the very low power of the transmitted images, of the order of  $100\mu W$ , so that photocurrents measured on small portions of the image are buried in the dark noise of the detection system. Phase sensitive amplification in type-I configuration, which has already produced impressive results in the single transverse mode case [23] is certainly a good candidate to produce measurable local quantum effects in an image. This would be interesting, not only for imaging, but also for their intrinsic quantum multimode properties, since they open the way to multiplexing of quantum information.

### acknowledgements

Laboratoire Kastler-Brossel, of the Ecole Normale Supérieure and the Université Pierre et Marie Curie, is associated with the Centre National de la Recherche Scientifique.

This work was supported by the European Commission in the frame of the QUANTIM project (IST-2000-26019).

### References

- [1] N. Treps, U. Andersen, B. Buchler, P.K. Lam, A. Matre, H. Bachor, C. Fabre, *Phys. Rev. Letters* **88**, 203601 (2002)
- [2] O. Jedrkiewicz, Y.-K. Jiang, E. Brambilla, A. Gatti, M. Bache, L. A. Lugiato, and P. Di Trapani *Phys. Rev. Lett.* **93**, 243601 (2004)
- [3] A. Gatti, E. Brambilla, M. Bache, and L. A. Lugiato, *Phys. Rev. A* **70**, 013802 (2004)
- [4] A. Heidmann, R. J. Horowicz, S. Reynaud, E. Giacobino, C. Fabre, and G. Camy, *Phys. Rev. Lett.* **59**, 2555 (1987)
- [5] S. Ducci, N. Treps, A. Maitre, and C. Fabre, *Phys. Rev.* **64**, 023803 (2001)
- [6] L. A. Lugiato, Ph. Grangier, *JOSA B*, Vol. **14** Issue 2 Page 225 (February 1997)
- [7] K.I. Petsas, A. Gatti, L.A. Lugiato, and C. Fabre, *Eur. Phys. J. D* **22**, 501-512 (2003)
- [8] M. Martinelli, N. Treps, S. Ducci, S. Gigan, A. Maitre and C. Fabre, *Phys. Rev. A*, **67**, 023808 (2003)
- [9] S.-K. Choi, M. Vasilyev, and P. Kumar, *Phys. Rev. Lett.* **83**, 1938 (1999)
- [10] E Lantz and F Devaux, *Quantum semiclass. Opt.* **9** 279-286 (1997)
- [11] J.A Levenson, I. Abram, T. Rivera and P. Grangier, *J. Opt. Soc. Am. B* **10**, 2233 (1993)
- [12] J. A. Levenson, I. Abram, T. Rivera, P. Fayette, J. C. Garreau, and P. Grangier, *Phys. Rev. Lett.* **70**, 267 (1993)
- [13] I. Protsenko, L. Lugiato, C. Fabre, *Phys. Rev* **A50**, 1627 (1994)
- [14] Sheng Feng, O. Pfister, *Phys. Rev. Lett.* **92**, 203601 (2004)

- [15] J. Laurat, T. Coudreau, G. Keller, N. Treps, C. Fabre, quant-ph/0410081
- [16] Black E.D., Am. J. Phys. **69** 79 (2001)
- [17] F. G. Colville , M. J. Padgett , and M. H. Dunn, Appl. Phys. Lett. **64** , 1490 (1994)
- [18] J. Teja and Ngai C. Wong, Optics Express **2**, 65 (1998)
- [19] B. Scherrer, I. Ribet, A. Godard, E. Rosencher, M. Lefebvre, JOSA B, **17** 1716 (2000)
- [20] G. A. Turnbull, D. McGloin, I. D. Lindsay, M. Ebrahimzadeh, M. H. Dunn, Optics Letters, Vol. **25** 341 (2000)
- [21] J.A. Arnaud, Applied Optics, Vol **8**. Issue 1, page 189 (1969)
- [22] S. Gigan, L. Lopez, N.Treps, A. Matre, C. Fabre, Image transmission through a stable paraxial cavity, Preprint.
- [23] T. C Ralph and P. K. Lam, Phys. Rev. Lett. 81, 5668 (1998)